



This is a repository copy of *Curcumin-mediated NRF2 induction limits inflammatory damage in, preclinical models of cystic fibrosis*.

White Rose Research Online URL for this paper:
<https://eprints.whiterose.ac.uk/id/eprint/225183/>

Version: Published Version

Article:

Leon-Icaza, S.A. orcid.org/0000-0002-7546-8228, Frétaud, M., Cornélie, S. orcid.org/0009-0005-6674-0794 et al. (8 more authors) (2025) Curcumin-mediated NRF2 induction limits inflammatory damage in, preclinical models of cystic fibrosis. *Biomedicine & Pharmacotherapy*, 186. 117957. ISSN 0753-3322

<https://doi.org/10.1016/j.biopha.2025.117957>

Reuse

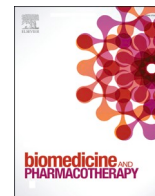
This article is distributed under the terms of the Creative Commons Attribution (CC BY) licence. This licence allows you to distribute, remix, tweak, and build upon the work, even commercially, as long as you credit the authors for the original work. More information and the full terms of the licence here:
<https://creativecommons.org/licenses/>

Takedown

If you consider content in White Rose Research Online to be in breach of UK law, please notify us by emailing eprints@whiterose.ac.uk including the URL of the record and the reason for the withdrawal request.



eprints@whiterose.ac.uk
<https://eprints.whiterose.ac.uk/>



Curcumin-mediated NRF2 induction limits inflammatory damage in, preclinical models of cystic fibrosis

Stephen A. Leon-Icaza^{a,1} , Maxence Frétaud^{b,1}, Sarahdja Cornélie^{c,1} , Charlotte Bureau^c, Laure Yatime^c , R.Andres Floto^d, Stephen A. Renshaw^e, Jean-Louis Herrmann^f, Christelle Langevin^g, Céline Cougoule^a, Audrey Bernut^{c,*} 

^a Institute of Pharmacology and Structural Biology, University of Toulouse, CNRS, Toulouse, France

^b Université Paris-Saclay, INRAE, Université de Versailles St Quentin, Virologie et Immunologie Moléculaires, Jouy-en-Josas, France

^c Laboratory of Pathogens and Host Immunity, University of Montpellier, CNRS, Inserm, Montpellier, France

^d Molecular Immunity Unit, University of Cambridge Department of Medicine, MRC-Laboratory of Molecular Biology, Cambridge, UK

^e The Bateson Centre, School of Medicine and Population Health, University of Sheffield, Sheffield, UK

^f Université Paris-Saclay, Université de Versailles St Quentin, Inserm, Infection et Inflammation, Montigny-le-Bretonneux, France

^g Université Paris-Saclay, INRAE, Infectiologie Expérimentale des Rongeurs et des Poissons, Jouy-en-Josas, France

ARTICLE INFO

Keywords:

Cystic fibrosis
Curcumin
NRF2
Inflammation
Oxidative response
Tissue repair
Zebrafish

ABSTRACT

Background: Overactive neutrophilic inflammation causes damage to the airways and death in people with cystic fibrosis (CF), a genetic disorder resulting from mutations in the *CFTR* gene. Reducing the impact of inflammation is therefore a major concern in CF. Evidence indicates that dysfunctional NRF2 signaling in CF individuals may impair their ability to regulate their oxidative and inflammatory responses, although the role of NRF2 in neutrophil-dominated inflammation and tissue damage associated with CF has not been determined. Therefore, we examined whether curcumin, an activator of NRF2, might provide a beneficial effect in the context of CF. **Methods:** Combining Cfr-depleted zebrafish as an innovative biomedical model with CF patient-derived airway organoids (AOs), we aimed to understand how NRF2 dysfunction leads to abnormal inflammatory status and tissue remodeling and determine the effects of curcumin in reducing inflammation and tissue damage in CF. **Results:** We demonstrate that NRF2 is instrumental in regulating neutrophilic inflammation and repair processes *in vivo*, thereby preventing inflammatory damage. Importantly, curcumin treatment restores NRF2 activity in both CF zebrafish and AOs. Curcumin reduces neutrophilic inflammation in CF context, by rebalancing the production of epithelial ROS and pro-inflammatory cytokines. Furthermore, curcumin improves tissue repair by reducing CF-associated fibrosis. Our findings demonstrate that curcumin prevents CF-mediated inflammation *via* activating the NRF2 pathway. **Conclusions:** This work highlights the protective role of NRF2 in limiting inflammation and injury and show that therapeutic strategies to normalize NRF2 activity, using curcumin or others NRF2 activators, might simultaneously reduce airway inflammation and damage in CF.

Abbreviations: AOs, airway organoids; AREs, antioxidant response elements; CDDO-Me, bardoxolone methyl; CF, cystic fibrosis; CFTR, cystic fibrosis transmembrane regulator; Csf3r, colony stimulating factor 3 receptor; DMSO, Dimethyl Sulfoxide; DpA, day post amputation; Dpf, day post fertilization; DPI, diphenyleneiodonium; DUOX, dual oxidase; ECM, extracellular matrix; HCFTR, human CFTR; HMOX1, heme oxygenase 1; HpA, hour post amputation; IL-1 β , interleukin 1 Beta; IL-8, interleukin 8; KEAP1, kelch-like ECH-associated protein 1; Mpa, minute post amputation; NADPH, nicotinamide adenine dinucleotide phosphate; Neh, Nrf2-ECH homology; NQO1, NADPH dehydrogenase quinone 1; NRF2, nuclear factor erythroid-derived 2; PBS, phosphate buffered saline; PI, propidium iodide; ROS, reactive oxygen species; SGH, second harmonic generation; TGF- β , transforming growth factor Beta; ZCfr, zebrafish Cfr.

* Corresponding author.

E-mail address: audrey.bernut@umontpellier.fr (A. Bernut).

¹ Equal contribution

<https://doi.org/10.1016/j.bioph.2025.117957>

Received 21 December 2024; Received in revised form 17 February 2025; Accepted 4 March 2025

Available online 31 March 2025

0753-3322/© 2025 The Author(s). Published by Elsevier Masson SAS. This is an open access article under the CC BY license (<http://creativecommons.org/licenses/by/4.0/>).

1. Introduction

Cystic fibrosis (CF) is a life-shortening disorder resulting from biallelic mutations in the CF transmembrane conductance regulator (*CFTR*) gene [1]. In lungs, *CFTR* defect results in an abnormal airway surface environment predisposing the individual to airway obstruction, infections and inflammation [1]. Inflammation is a natural response of host immunity to infection or injury. However, in CF, airway inflammation is both excessive and ineffective at clearing infections, causing progressive lung injury, ultimately contributing to respiratory impairment and death [2].

The characteristic feature of airway inflammation in CF is a disproportionate and sustained neutrophil-dominated phenotype [3]. Whether inherent to the *CFTR* defect or in response to infections, several cellular and molecular mechanisms have been proposed to explain the onset of neutrophilic inflammation in CF, including the pathogenic role of epithelial oxidative activity and excessive production of pro-inflammatory cytokines [3–5]. Interestingly, critical regulators of redox balance, such as the nuclear factor erythroid 2-related factor-2 (NRF2)-KEAP1 (Kelch-like ECH-associated protein 1) pathway, appear to be disrupted in several *in vitro* and *ex vivo* models of CF [6–9]. NRF2 plays a pivotal role in the lungs to mitigate oxidative and inflammatory responses through the regulation of genes involved in oxidative stress, antioxidant defense and pro-inflammatory processes via the antioxidant response elements (AREs) signaling pathway [10]. Although CF epithelia exhibit reduced NRF2 activity that has been associated with increased production of reactive oxygen species (ROS) and pro-inflammatory cytokines [6,7,9], it remains unclear whether neutrophilic inflammation is linked to defective NRF2 function in CF.

In CF care, the use of conventional anti-inflammatory therapies, such as corticosteroids and ibuprofen, can sometimes be effective in limiting inflammatory damage, but their adverse effects have discouraged their long-term use and new treatment options are needed [11]. Considering the protective role of NRF2, therapeutic strategies designed to activate NRF2 may have clinical benefit in CF by reducing oxidative stress, inflammation and subsequent cell damage in the lungs. Among the molecules activating the NRF2 pathway, curcumin, is known for its anti-inflammatory and antioxidant properties [12]. However, interestingly, although this compound is able to correct defects associated with $\Delta F508$ *CFTR* [13,14], the main mutation in CF, the biological significance of curcumin treatment in CF-related inflammatory damage is not known.

Using *Cftr*-depleted zebrafish larvae, as an innovative and relevant vertebrate model of CF [4,15], combined with CF patient-derived airway organoids (AOs) [7], we demonstrate that curcumin exposure, by normalizing NRF2 activity, can alleviate neutrophilic inflammation in the context of CF by reducing oxidative responses and the levels of pro-inflammatory cytokines. Moreover, curcumin can directly alleviate CF-associated tissue remodeling and allows tissue repair.

2. Materials and methods

2.1. Zebrafish husbandry and ethics statement

Zebrafish (*Danio rerio*) experiments described in the present study were performed by authorized staff and conducted by following the 3Rs -Replacement, Reduction and Refinement- principles in compliance with the European Union guidelines for handling of laboratory animals. Breeding and maintenance of adult fish were performed in the Bateson Centre (University of Sheffield, Sheffield, UK; license number P1A4A7A5E), the IERP (Inrae, Jouy-en-Josas, France; license number C78–720) and the ZEFIX-Lphi (CNRS, University of Montpellier, Montpellier, France; license number CEEA-LR-B34–172–37) fish facilities, according to the local animal welfare standards set approved by the UK Home Office under Animal Welfare and Ethical Review Body, the Directions Sanitaires et Vétérinaires de Versailles et de l'Hérault, the

Comités d'Ethiques pour l'Expérimentation Animale de Paris-Saclay et de la région Languedoc Roussillon (France) and the French Ministry of Agriculture and Food.

Experimental procedures were performed using the pigment-less *nacre* [16] or golden [17] lines along with the following transgenic lines: *TgBAC(mpx:eGFP)i114* [18] to label neutrophils; *Tg(il1 β :eGFP-F)ump3* [19] to visualize the transcriptomic expression of *il1 β* ; *Tg(rcn3:gal4)^{pd1023}* and *Tg5(UAS:mCherry)^{pd1112}* referred to as *Tg(rcn3:gal4/UAS:mCherry)* to label mesenchymal cells [20].

All zebrafish experiments were performed on larvae < 5 days post-fertilization (dpf). The number of animals used for each procedure was guided by pilot experiments or by past results [4,21]. Zebrafish eggs were obtained from pairs of adult fish by natural spawning and raised in E3 water [22] at 28°C and exposed on a 14:10 hours light/dark cycle to maintain proper circadian conditions. For zebrafish anesthesia procedures, larvae are immersed in a 168 mg/L tricaine (Sigma-Aldrich) or 0.0075% eugenol (Fisher Scientific) solution in E3 water. When required, larvae were euthanized using an overdose of tricaine (500 mg/L).

2.2. Morpholino injections

Morpholinos used in this study were purchased from Gene Tools. The morpholinos for *cftr* knock-down (5'-GACACATTTGGACACCA-CACAA-3'), *nrf2a* knock-down (5'-CATTTCAATCTCCATCATGTCT-CAG-3'), *nrf2b* knock-down (5'-AGCTGAAAGTCTGCCATGTCTTCC-3') and *il1 β* knock-down (5'-CCCACAACTGCAAAATATCAGCTT-3') were prepared and injected into one-cell-stage zebrafish as previously described [15,19,23]. For the selective depletion of neutrophils into zebrafish larvae, the *csf3r* morpholino (5'-GAAGCACAAGCGAGACGGATGCCAT-3') targeting the *csf3* gene was used [24]. A standard control morpholino (5'-CCTCTTACCTCAGTTACAATTTATA-3') was used as a negative control.

2.3. Drug treatments in zebrafish larvae

To explore the therapeutic efficacy of curcumin, zebrafish larvae were incubated in sterile E3 medium supplemented with 2.5 μ g/mL of curcumin (Sigma-Aldrich). Both ML 385 (Sigma-Aldrich) and bardoxolone methyl (CDDO-Me) (Sigma-Aldrich) were used at 1.5 μ g/mL working concentration to reciprocally inhibit or activate Nrf2 signaling in zebrafish. Initial assays were conducted to identify optimal and non-toxic dosages to use for curcumin, ML385 and CDDO-Me. Oxidative activity was blocked using 100 μ g/mL of diphenyleneiodonium (DPI, Sigma-Aldrich) as described earlier [25]. Dimethyl sulfoxide (DMSO, Sigma-Aldrich) was used as vehicle control.

2.4. RNA Isolation from Zebrafish larvae and qRT-PCR analysis

Total RNA from pools of 10–15 larvae per biological experiment were extracted using the Nucleospin RNAII kit (Macherey-Nagel) at the time points indicated in the Figure legends and cDNA synthesized with the M-MLV reverse transcriptase (Invitrogen). Real-time RT-PCR were performed using a SensiFAST SYBR Green No-ROX mix (Thermo Fisher Scientific) on a LightCycler 480 instrument (Roche) as described [26] and gene expressions were detected with the gene-specific primers provided in Table S1. Each experiment was run in triplicate. Δ CT were calculated using the housekeeping gene *ef1 α* as a reference gene. Relative expression levels were calculated using the $2^{-\Delta\Delta CT}$ method.

2.5. Inflammation assays in zebrafish larvae

Inflammation was elicited by distal or proximal tail fin amputation on 3 dpf anesthetized larvae using a microscalpel (5 mm depth; World Precision Instruments) according to established procedures [4,18].

Neutrophil response was observed and evaluated by manually

assessing the number of cells at wound sites at relevant time points using a fluorescence dissecting stereomicroscope (Leica) as previously defined [4]: 2 hours post-amputation (hpA) (acute phase of neutrophil response), 4 hpA (neutrophil recruitment peaking) or 8 hpA (resolution phase of neutrophil response). Neutrophils at the wound sites were imaged on an Eclipse TE2000 U inverted compound fluorescence microscope (Nikon UK Ltd., Kingston upon Thames, UK) equipped with a 20x NA objective lens, using a 1394 ORCA-ERA camera (Hamamatsu Photonics Inc). Overlays of fluorescent and DIC images were assembled using FIJI (National Institutes of Health).

Epithelial *il1 β* expression at the wound sites (50 μ m anterior from the wound margin) was observed and captured at 2 hpA, using an Olympus MVX10 fluorescence microscope (Olympus, Life Science) equipped with a X-Cite Xylis LED (Excelitas Technologies) light source. Images were acquired with a Hamamatsu ORCA-spark Digital CMOS C11440-36U camera (Hamamatsu Photonics Inc) and processed using Olympus CellSens Standard 3.1 software (Olympus, Life Science). *il1 β* activity was assessed in FIJI using the intensity of fluorescence and normalized to uninjured larvae (control or morphant animals; untreated or treated animals).

2.6. Oxidative activity assay in zebrafish larvae

Epithelial oxidative response was detected using CellROX® deep red or CellROX® green (Thermo Fisher Scientific) following protocol previously established [4] and elicited by tail fin amputation as described above or by laser-mediated injury [21].

For tail fin amputation procedure, following CellROX® green staining, larvae were injured then ROS production at the wound sites (50 μ m anterior from the wound margin) was observed and captured at 30 minutes post-amputation (mpA) using fluorescence microscope (Olympus, Life Science). For laser injury, following CellROX® deep red staining, anaesthetized larvae were mounted in 0.8 % low melting point agarose (Thermo Fisher Scientific). A femtosecond titanium:sapphire pulsed laser (Coherent Vision II) set at 800-nm and at 40 % laser power was used to injure caudal fin. A 9.23 μ m x 9.23 μ m field of view was scanned during 1 second with a pixel well time of 72 ns using an upright Leica SP8 confocal microscope equipped with an HCX IRAPO 25X/0.95NA water immersion objective (Leica Microsystems). The laser makes a small circular injury to tissue resulting in the production of ROS and accumulation of neutrophils in this area [21]. ROS production at the wound sites was immediately time-lapsed at indicated time points throughout acute inflammatory stage. CellROX® deep red was excited with a 633 nm laser, then fluorescence and bright field transmission images were acquired with a with photomultiplier tube detectors and processed using LASX software (Leica). Oxidative activity was assessed in FIJI using the intensity of fluorescence and normalized to uninjured larvae (control or morphant animals; untreated or treated animals).

2.7. In vivo tissue repair assay

Tissue repair assay was performed following established methods [4]. Briefly, 2 dpf embryos were anesthetized then tail fin amputated at the boundary of the notochord without injury to the notochord (distal injury). Tissue repair performances were evaluated by assessing the regenerated tail fin areas/lengths/widths and wound contour lengths at 3 days post-amputation (dpA) under a stereomicroscope (MZ10F, Leica Microsystems) equipped with a PLANAPO 1X objective lens. Images were acquired with a MC170HD camera (Leica), then processed and analyzed with FIJI: regrowth areas were measured by outlining the total fin tissue area distal to the notochord using the polygon tool, regrowth lengths and widths were measured by using the straight-line tool. Percentages of regeneration were calculated by normalizing the regenerated tail fin areas/lengths/widths *versus* fin areas/lengths/widths of unamputated animals (control or morphant animals). To assess the length of wound edge as an indicator of projections, the length of the

wound edge was measured using the freehand line tool to trace the contour of the wound edge, as previously described [27].

2.8. Second harmonic generation microscopy and collagen fiber observation

Second harmonic generation (SHG) imaging was performed on living zebrafish larvae mounted in 0.8 % low-melting agarose, using an upright Leica SP8 two-photon microscope equipped with an HCX IRAPO 25X/0.95NA water immersion objective (Leica Microsystems). Caudal fin areas were excited at 1040 nm with a Chameleon Vision II laser (Coherent). SHG signal, corresponding to collagen fibers, was detected in a non-descanned (NDD) pathway with a hybrid detector (HyD, Leica) associated with a 525/50 nm bandpass filter (green channel). Images of regenerated fins were acquired with photomultiplier tube detectors and processed using LASX software (Leica). Overlays of fluorescent and Brightfield images, and maximal projections of image stacks were assembled using FIJI. 3D reconstructions were produced using Imaris 9.0 software (Bitplane).

Collagen fiber quantification. Collagen alignment quantifications were performed using the collagen quantification platform CurveAlign 4.0 [28].

Area devoid of collagen fibers. To measure the areas between the wound tissue edge and the ends of the SHG detected fibers, maximum projections of SHG z-stacks, with the notochord vertically centered, were generated. A freehand line was drawn along the ends of the fibers and applied to the corresponding brightfield image, then the area between this fiber-end boundary and the wound edge was drawn and measured using FIJI software.

2.9. Human bronchiolar airway organoid ethics statement, preparation and treatments

The acquisition of patient data and lung tissue for human bronchiolar AOs generation was performed in accordance with the Medical Research Involving Human Subjects Act and approved by the CHU of Toulouse and the CNRS under the number agreements CHU/19244 C and CNRS/205782. Healthy tissue from two volunteers with lung cancer and lung biopsies from two consented patients with CF (Table S2) were used to derive AOs as previously described [7,29,30].

To explore the therapeutic efficacy of curcumin, healthy-AOs and CF-AOs were embedded in 40 μ l drops of Cultrex growth factor reduced basement membrane extracts (BME) type 2 (R & D Systems), and seeded on Nunclon Delta surface 24-well plates (Thermo Fisher Scientific). Once the Cultrex has polymerized, 500 μ l of AO complete media, without N-acetylcysteine and without antibiotics, were added. According to the indicated conditions, AOs were stimulated or not with 30 μ M curcumin for 1 or 4 days. The doses of curcumin we identified that did not generate toxicity.

2.10. Human bronchiolar airway organoid mortality assay

To determine AO mortality, healthy-AOs and CF-AOs stimulated or not for 4 days with 30 μ M curcumin were stained with 50 μ g/mL Propidium Iodide (PI, Thermo Fisher Scientific) as previously described [7]. PI incorporation was then immediately analyzed by live imaging using an EVOS M7000 Imaging System (Thermo Fisher Scientific) (10x, at 37°C with 5 % CO₂) and cellular death was assessed in FIJI using the intensity of fluorescence.

2.11. Human bronchiolar airway organoid epithelial thickness

Healthy-AOs and CF-AOs were embedded in a Cultrex matrix, then seeded and cultivated for a minimum of five weeks on Nunclon Delta surface 24-well plates, utilizing complete AO media. The AOs were maintained at 37°C with 5 % CO₂. Upon completion of the cultivation

period, the AOs were either treated with 30 μ M of curcumin for 4 days or left untreated. Following this treatment, bright-field images of each well were acquired using an EVOS M7000 Imaging System (10x magnification), and subsequently, the analysis of epithelial thickness for each AO was conducted using the FIJI software.

2.12. RNA isolation from human bronchiolar airway organoids and qRT-PCR analysis

Healthy- or CF-AOs (~15 per condition) stimulated or not with 30 μ M curcumin for 1 day, were harvested with cold 1X phosphate-buffered saline (PBS). The AOs collected were centrifugated at 800 g x 5 minutes, and the supernatants were discarded. Total RNA was extracted using the RNeasy mini kit (Qiagen), followed by retro-transcription (150 ng) with the Verso cDNA Synthesis Kit (Thermo Fisher Scientific). mRNA expressions were evaluated with an ABI 7500 real-time PCR system (Applied Biosystems) and the SYBR™ Select Master Mix (Thermo Fisher Scientific). Relative quantifications were determined by the $2^{-\Delta\Delta Ct}$ method and normalized to GAPDH. Primer sequences are provided in Table S1.

2.13. 3D-modeling and structural analysis

The 3D structural models for the zebrafish *nrf2a* and *nrf2b* were predicted using AlphaFold (v2.3.2) [31] from the online Colab

notebook. Structural alignment was done in Coot [32] and all figures were made with the Pymol Molecular Graphics System (version 0.99rc6, DeLano Scientific LLC). Sequence alignment were done in Clustal Omega [33] and sequence conservation was analyzed with ALINE [34].

2.14. Quantification and statistical analysis

Statistical analysis was performed using Prism 10.0 (GraphPad Software) and detailed in each Figure legend. ns, not significant ($p \geq 0.05$); * $p < 0.05$; ** $p < 0.01$; *** $p < 0.001$; **** $p < 0.0001$.

3. Results

3.1. Zebrafish and human NRF2 proteins are structurally conserved

Two putative co-orthologs of human NRF2 (hNRF2) have been described in zebrafish, *Nrf2a* and *Nrf2b* [23,35]. Sequence comparison revealed that *Nrf2a* resembles hNRF2 more closely than *Nrf2b* as it shares 46% sequence identity with the human protein and displays a similar domain organization, with seven Neh (NRF2-ECH homology) domains and highly conserved consensus motifs, in particular in the Neh1 (ARE-binding) and Neh2 (KEAP1-binding) domains (Fig. 1A; S1). In contrast, *Nrf2b* diverges a bit more from the human protein, with only 32% sequence identity, long deletion regions and only six conserved Neh domains (Fig.S1; S2A). Despite some degree of conservation,

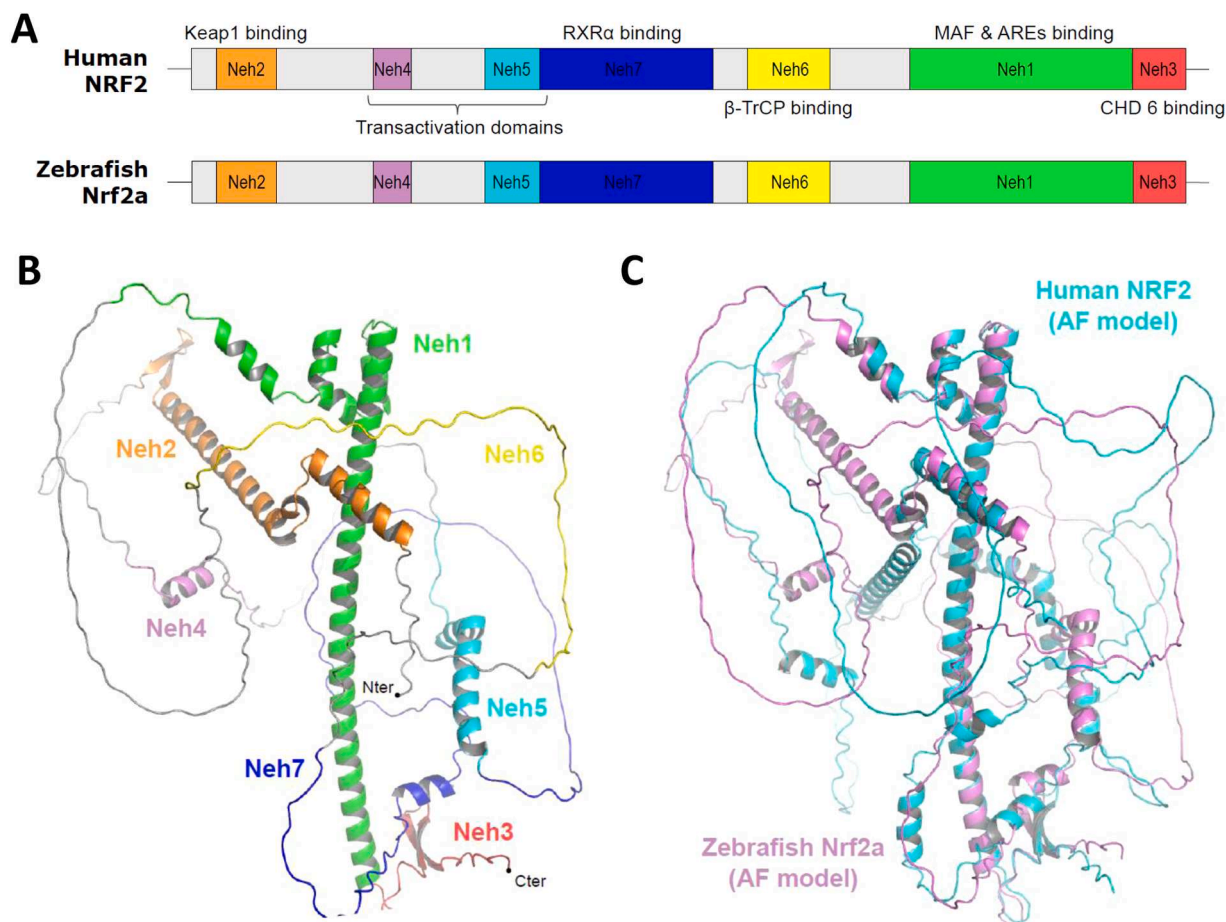


Fig. 1. Structural analysis of zebrafish Nrf2a and comparison with human NRF2. (A) Domain organization of human NRF2 (hNRF2), with the target binding partners indicated for each domain, and predicted domain organization for zebrafish Nrf2a. All seven Neh domains seem to be present in Nrf2a. (B) 3D-structure of zebrafish Nrf2a predicted with AlphaFold. In this model, long unstructured regions alternate with shorter regions adopting defined secondary structures, mostly α -helices. The Neh domains are represented with the same color code as in panel A. (C) Structural overlay of the AlphaFold-predicted model for zebrafish Nrf2a (light purple) with that of hNRF2 (cyan). The position of the secondary structure elements within the Nrf2a model matches well with those predicted for hNRF2.

sequence identity remains medium between hNRF2 and the zebrafish Nrf2a and Nrf2b, which questions the true functional orthology between these proteins.

To further address their resemblance, we performed structural analysis of the three proteins using AlphaFold [31]. As shown in Fig. 1B, Nrf2a is proposed to adopt a largely unstructured 3D-architecture, alternating long coiled-coil regions with shorter, well-structured domains that correspond to the functional core of the Neh domains and are predicted with high confidence. In contrast, the low confidence of the prediction for coiled-coil regions suggests that they may fold differently when interacting with binding partners. Comparison of the AlphaFold model of Nrf2a with that of hNRF2 (Fig. 1C) reveals a high structural similarity. In particular, the predicted secondary structure elements are placed at the same position in Nrf2a and hNRF2. A similar structural analysis was performed on Nrf2b and predicts a closely related structural organization although slightly more divergent than hNRF2 (Fig. S2B-C). Taken together, these data suggest that zebrafish Nrf2 proteins, and in particular Nrf2a, are structural homologs of hNRF2. This high resemblance gives strong confidence that the proteins will function similarly in both organisms and thus validates the use of zebrafish model to study the function of NRF2 *in vivo*.

3.2. CF-mediated NRF2 deficiency promotes overactive inflammation *in vivo*

To better understand the impact of dysfunctional CFTR on NRF2 activity *in vivo*, the expressions of *nrf2a* and *nrf2b* in control and Cfr-depleted (*cfr* morphant) zebrafish larvae were first evaluated following injury-induced inflammation (Figs. 2A, [4]). While injury consistently triggered *nrf2a* response in control larvae, RT-qPCR analyses revealed a significant downregulation of *nrf2a* expression in CF animals (Fig. 2B). Conversely, we found that Cfr deficiency resulted in increased expression of *nrf2b* compared to the normal condition (Fig. 2B).

Next, to determine how NRF2 defect might contribute to the hyper-inflammatory state in CF, expression of *nrf2a* and/or *nrf2b* were knocked-down in zebrafish using established morpholinos [23]. As an overactive neutrophil response is the hallmark of CF-related inflammation, we first investigated the consequence of Nrf2 inhibition on neutrophil mobilization post-injury using a reporter line labelling neutrophils [18]. Only larvae injected with the *nrf2a* morpholino exhibited an increased neutrophil mobilization to the wound compared to those injected with the control one, while no significant change was observed from animals injected with the *nrf2b* morpholino (Fig. 2C-D; S3A-B). These results suggest that Nrf2a acts as a main regulator of neutrophilic inflammation in zebrafish, whereas Nrf2b shows no obvious function. Importantly, a similar increase in the number of wound-associated neutrophils was observed in Cfr- and Nrf2a-depleted larvae, and in the double Cfr/Nrf2a, Cfr/nNrf2b and Cfr/Nrf2a+b-depleted animals (Fig. 2E). This is consistent with the hypothesis that NRF2 signaling is already disrupted in CF and might be involved in the neutrophilic inflammation seen in this disease. We furthermore modulated NRF2 activity pharmacologically using the NRF2 blocker ML385 or the NRF2 activator CDDO-Me. Corroborating our finding using genetic approaches, we also observed that ML385 markedly exacerbated neutrophil response in wild-type animals (Fig. 2F). In contrast, a protective effect of CDDO-Me exposure, acting to reduce neutrophilic inflammation, was demonstrated in CF larvae (Fig. 2F).

ROS generation by the DUOX NADPH oxidases is known to induce neutrophil response [36]. As shown in Fig.S4A-B, pharmacological inhibition of ROS production reduced neutrophilic inflammation in Nrf2a-depleted zebrafish, suggesting that exaggerated neutrophil mobilization associated with the loss of Nrf2a is due to a disrupted oxidative activity. To explore this hypothesis, we next addressed whether Nrf2a ablation could affect oxidative responses in zebrafish. As expected, Nrf2a deficiency caused an abnormal elevation of ROS production at the wound (Fig.S4C-D), coinciding with increased expression

of *duox* (Fig. 2G). In contrast, *nqo1* and *hmx1*, two anti-oxidative NRF2 target genes, were downregulated in animals lacking Nrf2a (Fig. 2G). Moreover, we found that loss of Nrf2a led to increased expression of *il8* and *il1 β* (Fig. 2G; S4E-F), two other mediators of neutrophil chemotaxis (Figs.S4G, [4]) that can be regulated by NRF2 [37].

Collectively, these observations provide evidence that NRF2 signaling is necessary to coordinate neutrophil trafficking. In particular, we show that Cfr-depleted zebrafish recapitulate the abnormal NRF2 status associated with CF and support that dysfunctional NRF2 activity in CF airways contributes to neutrophilic inflammation, likely by causing deleterious changes in oxidative and pro-inflammatory responses.

3.3. CF-mediated NRF2 deficiency alters tissue repair *in vivo*

Our previous work revealed that Cfr-depleted zebrafish exhibit impaired tissue repair after injury [4]. Given the role of the NRF2 signaling pathway in repair processes [38], we next investigated whether dysfunctional NRF2 activity might impede tissue repair in the context of CF. Since zebrafish caudal fins undergo complete regeneration after amputation, we assessed zebrafish regenerative performances in the absence of Nrf2 signaling by quantifying fin regrowth post-amputation (Figs. 3A, [4]). Fin regrowth was impaired in Nrf2a-depleted zebrafish compared to controls, in association with a reduction in the area, length and width of regenerated fins (Fig. 3B-C), whereas the loss of Nrf2b did not affect regrowth (Fig.S5). These findings indicate that Nrf2a is the likely NRF2 paralogue mediating tissue repair process in zebrafish. Importantly, similar regenerative defects were observed in both *cfr* and *nrf2a* morphants, and in the double *cfr/nrf2a* morphants (Fig. 3D), suggesting that impaired tissue repair in CF zebrafish could be linked to defective Nrf2a. We next reasoned that excessive neutrophil response at wound (Fig. 2) might contribute to impaired tissue repair in Nrf2a-depleted zebrafish. To address this question, we ablated neutrophils in zebrafish using the *csf3r* morpholino [24]. As shown in Fig.S6, removal of neutrophils improved fin regrowth in *nrf2a* morphants.

NRF2 influences extracellular matrix (ECM) deposition and remodeling, including collagen formation [39], a critical step during tissue repair. In zebrafish, collagen projections at the wound edge guide epithelial growth during fin regeneration and initiate tissue repair ([27]; Fig. 3E). Since tissue repair requires a functional NRF2 activity, we sought to characterize the effect of Nrf2 ablation on the formation of collagen projections during fin regrowth. Using second harmonic generation (SHG) imaging to visualize collagen fibers, we found that the formation of collagen projections was disrupted in Nrf2a-deficient larvae (Fig. 3F-I). While the wound edges in control animals formed uneven borders containing collagen associated-epithelial projections, Nrf2a-depleted larvae displayed smooth wound edges and relative absence of such projections (Fig. 3F-H). In addition, the contour of the wound edges was measured as a marker of collagen fiber formation [27]. The Nrf2a-deficient larvae had shorter contour lengths at the wound edges as compared to control animals (Fig. 3I). These observations indicate that Nrf2a deficiency impairs tissue repair in zebrafish, by affecting the formation of collagen and epithelial projections.

Altogether, these findings provide evidence that NRF2, by regulating collagen formation, is required for tissue repair, and support the proposal that NRF2 deficiency in CF airways could be involved in the abnormal tissue remodeling seen in this disease [40].

3.4. Curcumin-induced Nrf2 activation reduces CF-related inflammation in zebrafish

Since NRF2 signaling represents an important mechanism in the regulation of inflammatory and tissue repair processes, it could be considered as a promising therapeutic target to prevent inflammation and tissue damage in CF. We therefore examined whether curcumin, a

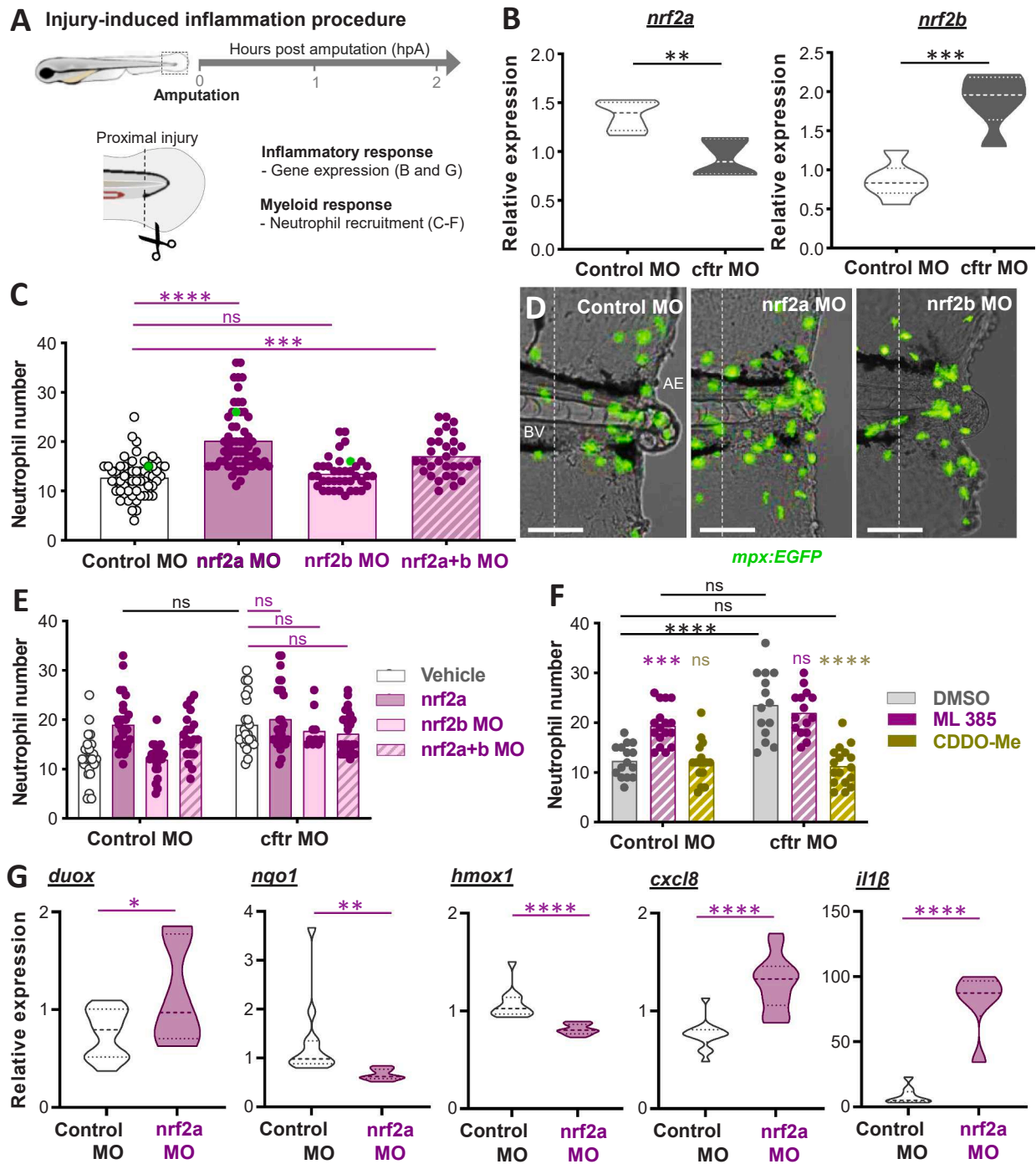
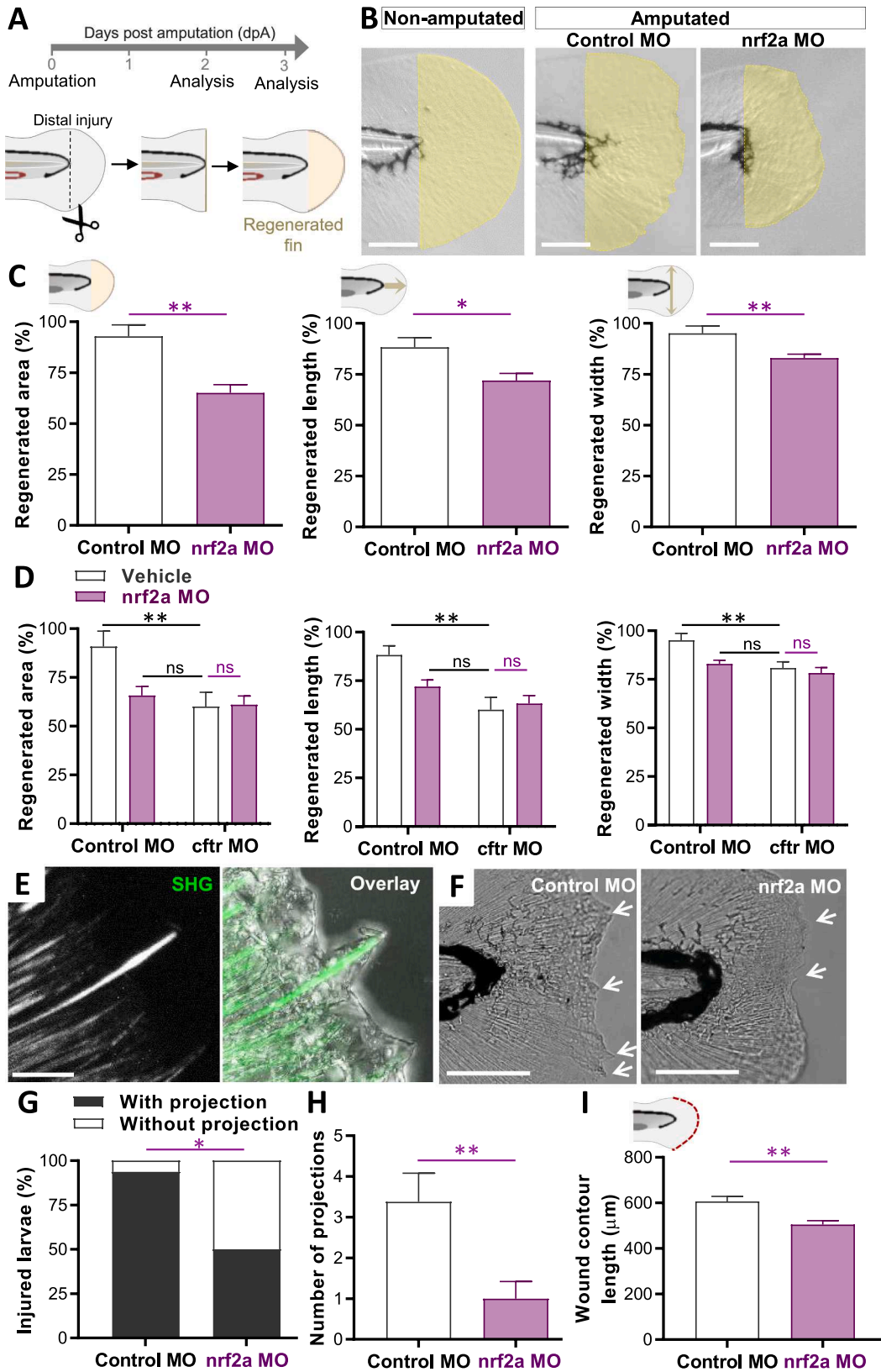


Fig. 2. Injury-induced inflammatory responses are exacerbated in the absence of Nrf2 signaling in zebrafish larvae. (A) Schematic of injury-induced inflammation assay and analyses. Caudal fin amputations (dotted lined) were performed proximally through the notochord (N) at 3 days post-fertilization (dpf). (B) Control (control morphant (MO)) and *cftr* MO (generated using the validated *cftr* morpholino [15]) were caudal fin amputated then the level expressions of mRNA for *nrf2a* (left) and *nrf2b* (right) genes are evaluated at 2 hours post-amputation (hpA) by RT qPCR. Graphs showing the fold change over total tissue from uninjured larvae (relative gene expression from at least 3 independent experiments performed in triplicates, mean and quartiles shown, Two-tailed Student *t*-test). (C–E) Neutrophil mobilization to tissue injury in the neutrophil-specific *TgBAC(mpx:EGFP)i114* line [18] is observed and enumerated at 2 hpA under a fluorescence microscope. The neutrophil count area is defined as the region between the blood vessels (BV) end and the amputation edge (AE). (C) Number of neutrophils mobilized to the wound in control MO, *nrf2a* MO, *nrf2b* MO or double *nrf2a* MO / *nrf2b* MO (*nrf2a+b* MO). Each dot represents the number of neutrophils at the wound in a single larva (3 independent experiments, One-way ANOVA with Dunnett's comparisons test). (D) Representative images of injured tails (scale bars, 100 μ m). The images are denoted as green data points in (C). (E) Inhibition of *nrf2a*, *nrf2b* or *nrf2a+b* was carried out in control and CF animals by injecting the *nrf2a* morpholino, the *nrf2b* morpholino or the *nrf2a* + *nrf2b* morpholinos reciprocally. Neutrophil recruitment assay (3 independent experiments, Two-way ANOVA with Tukey's multiple comparisons test). (F) Control MO and *cftr* MO *TgBAC(mpx:EGFP)i114* were treated with the NRF2 inhibitor ML 385, the NRF2 agonist CDDO-Me or DMSO as mock control prior to caudal fin amputation procedure, then injured and immediately put back in treatments. Neutrophil number at injured tails were enumerated at 2 hpA (3 independent experiments, Two-way ANOVA with Tukey's multiple comparisons test). (G) Relative expression of mRNA for *duox*, *cxcl8* and *il1β* at 2 hpA (*duox*, *cxcl8* and *il1β*) or 8 hpA (*nqo1* and *hmxo1*) were determined by RT qPCR. (from at least 3 independent experiments performed in triplicates, mean and quartiles shown, Two-tailed Student *t*-test).



(caption on next page)

Fig. 3. Nrf2a-depleted zebrafish exhibit reduced tissue repair responses after injury. (A-I) Tissue repair performance assessment. Caudal fin amputations were performed without injury to the notochord (dotted line) at 2 dpf, then the potential of tissue repair was evaluated at 2 (E-I) or 3 (B-D) days post-amputation (dpA). (B-C) Control MO and *nrf2a* MO were caudal fin amputated. Representative imaging of injured tail fin (scale bars, 100 μ m) (B) and measurement of regenerated fin areas, lengths and widths (C) (n = 14–18 from 3 independent experiments, Two-tailed Student *t*-test). Error bars represent standard error of the mean (SEM). The regenerated fin areas were defined as the region between the amputation edge and the end of the extended fin. The regenerated fin lengths were measured from the notochord tip to the end of the extended fin. The regenerated fin widths were defined as the max width measured from the amputation edge to the end of the extended fin. (D) Inhibition of *nrf2a* was carried out in WT and CF animals by injecting the *nrf2a* morpholino. Measurement of regenerated tail fin areas, lengths and widths in the presence or absence of *nrf2a* (n = 16 from 3 independent experiments, Two-way ANOVA with Tukey's multiple comparisons test). (E) SHG and high magnification bright field imaging showing epithelial projection associated with collagen fibers (scale bar, 10 μ m). (F) Representative bright field microscopy of injured caudal fin showing extended collagen fiber-containing epithelial projections (arrows) pushing the healing plane forward (scale bars, 100 μ m). Morpholino knockdown of *nrf2* expression reduced the appearance of projections, suggesting that Nrf2a modulates the formation of collagen fiber in zebrafish. (G) Proportion of larvae forming visible projections (G; n = 14–16, Fisher test). \approx 90 % of control larvae had visible projections, compared to only \approx 50 % of *nrf2a* MO. (H) Mean \pm SEM number of projections per larvae (H; n = 14–16, Two-way ANOVA, Tukey's multiple comparisons test). (I) Measurement of wound contour length in the presence or absence of *nrf2a* (n = 14–18 from 3 independent experiments, Two-way ANOVA with Tukey's multiple comparisons test). Nrf2a deficiency impairs tissue repair in zebrafish by affecting the formation of collagen and epithelial projections.

NRF2 activator, might provide a beneficial effect in the context of CF (Fig. 4A).

Firstly, we confirmed that curcumin rescued disrupted *nrf2* expressions in *Cftr*-depleted zebrafish (Fig. 4B; S7) and could promote Nrf2a activation. Curcumin efficiently reduced early neutrophil response to injury in CF larvae compared to DMSO-treated animals (Fig. 4C-D; S8). To validate the NRF2-targeted action of curcumin, we knocked-down *nrf2a*, *nrf2b* or *nrf2a+b* expression in zebrafish and examined whether curcumin was still able to restore normal neutrophil responses in the absence of Nrf2 signaling. Although wound-associated neutrophil number was higher in Nrf2a-depleted larvae than control animals when treated with curcumin, the treatment partially reduced neutrophilic inflammation in the absence of Nrf2a (Fig.S9). However, when both *nrf2a* and *nrf2b* were depleted, curcumin failed to reduce neutrophilic inflammation, supporting the notion that curcumin regulates neutrophil responses through Nrf2-dependent mechanisms. Importantly, when *nrf2a* was depleted in CF animals, curcumin failed to alleviate inflammation (Fig. 4E), confirming that the presence of functional Nrf2 proteins, at least Nrf2a, is required for the anti-inflammatory action of curcumin to occur in the context of CF.

We next sought to identify the mechanisms by which curcumin-induced NRF2 activation acts to reduce neutrophilic inflammation in CF animals. Since exaggerated production of ROS by epithelia contributes to the neutrophilic inflammation in CF [4,5], we first proceeded to examine the benefits of curcumin in reducing oxidative response in *Cftr*-depleted larvae. Unexpectedly, rapidly after injury, curcumin-treated animals exhibited a strong oxidative burst at the wound (Fig. 4F-H). However, while oxidative responses increased over time in DMSO-treated animals, curcumin gradually reduced ROS signal, suggesting that curcumin treatment might reduce ROS generation through the modulation of NRF2-induced genes. As expected, the anti-oxidative action of curcumin was confirmed by the downregulation of *duox* and the upregulation of *nqo1* genes in CF larvae treated with curcumin (Fig. 4I-K). Moreover, curcumin reduced the increased *Il8* and *Il1 β* activity caused by CF, as demonstrated by RT-qPCR and/or microscopy analyses (Fig. 4L-O; S10A-D).

Together these data indicate that curcumin alleviates CF-related neutrophilic inflammation, by reducing oxidative and pro-inflammatory responses, via NRF2 activation.

3.5. Curcumin prevents tissue damage by improving tissue remodeling and repair in CF zebrafish

We next investigated whether curcumin-induced Nrf2a activation could rescue abnormal tissue remodeling and repair in CF zebrafish [4].

As shown in Fig. 5A-C, curcumin significantly improved tissue repair in CF injured zebrafish. Next, we sought to determine whether impaired fin regeneration in CF zebrafish was associated with a defect in collagen remodeling. Comparative analysis of the control and *Cftr*-depleted zebrafish regenerated tissue revealed that collagen fibers did not

project well in CF animals (Fig. 6A-D; S11A). Furthermore, SHG imaging showed that collagen fibers were completely disrupted upon injury in CF animals, as measured by the areas devoid of fibers (Fig. 6E-G; S11B). Fiber alignment analysis (Fig. 6H-L) indicated that these changes correlated with a diminished number of fibers (Fig. 6I) and a reduction in their lengths (Fig. 6J). Interestingly, significant change in collagen fiber widths was seen in *cftr* morphants, with thicker fibers compared to control morphants (Fig. 6K). Importantly, this change was associated with an overexpression of the transforming growth factor- β (Tgf- β) (Fig. 6L), a driver of fibrosis in CF [41]. The population of fibers in CF fins also tended to be less perpendicular overall to the wound edge than their control counterparts (Fig. 6M). Overall, regenerated tissues in CF animals consistently showed unaligned fibers compared to control, and were more prone to develop aberrant fiber extrusions into the intra-fiber space (Fig. 6N). Interestingly, while mesenchymal cells are essential to guide the collagen fibers organization in zebrafish fins [42], we observed that disrupted fiber content and orientation coincided with an abnormal mesenchymal cell distribution (Fig.S11C). Remarkably, all these aberrant phenotypes are rescued by curcumin treatment (Fig. 6; S11).

Together these data indicate that curcumin improves tissue repair and prevents tissue damage in CF animals, by restoring remodeling of collagen fibers.

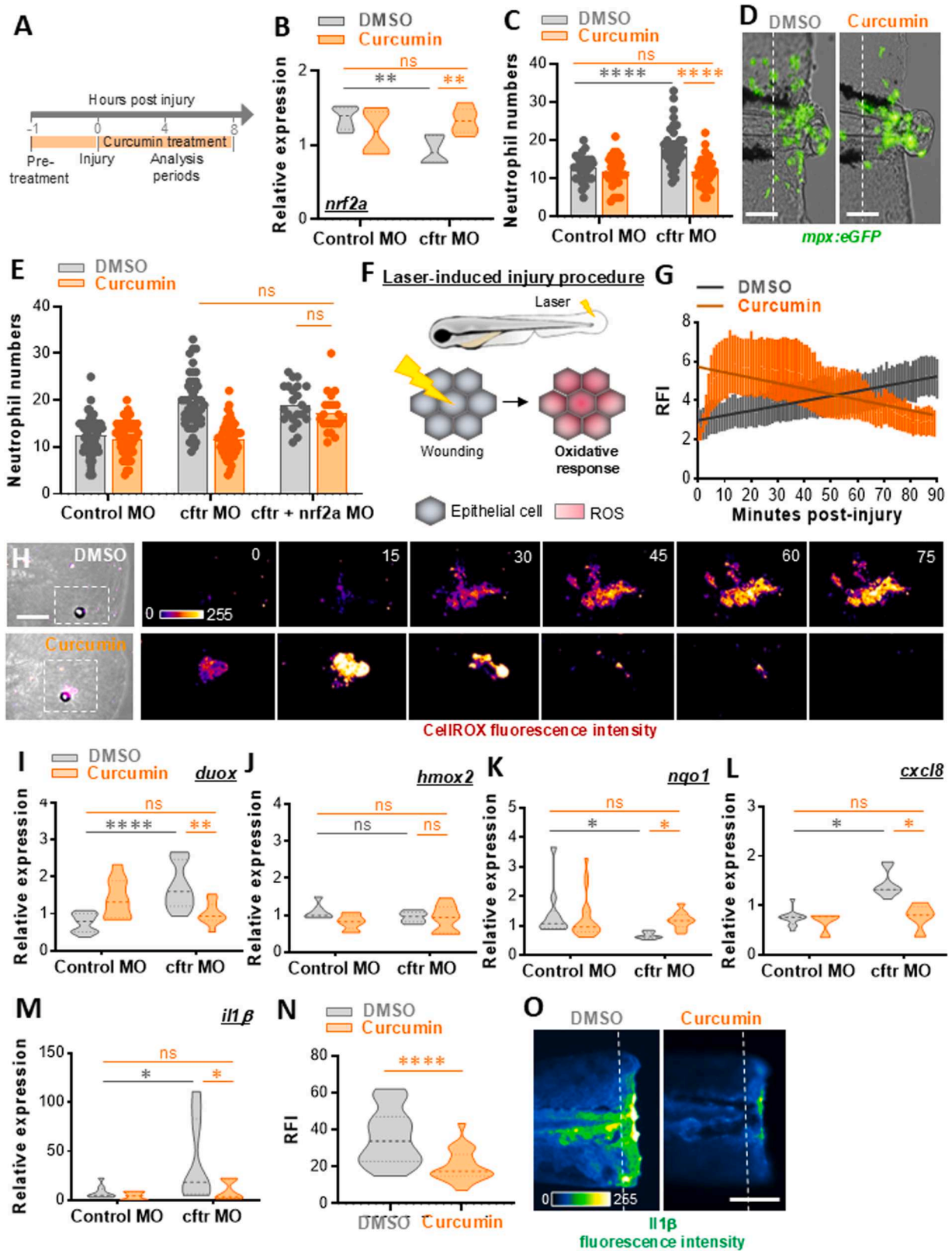
3.6. Curcumin reduces inflammation and epithelial damage in CF patient-derived airway organoids

Finally, to further confirm the efficacy of curcumin in both reducing inflammation and tissue damage in CF, we validated the effect of curcumin treatment into a human system using bronchiolar AOs-derived from patients with and without CF [7,30].

While CF-driven dysfunctional NRF2 activity was confirmed by the reduction in expression of *NRF2* in CF-AOs compared to healthy-AOs [7], we first showed that curcumin increased *NRF2* expression in CF-AOs (Fig. 7A). Importantly, curcumin brought *IL1 β* and *IL8* expression back to normal level in CF-AOs (Fig. 7B) and mitigated oxidative response in association with reduced expression of *DUOX1* and higher expression of *NQO1* (Fig. 7C).

As previously described, CF-AOs display increased cell death and thicker epithelium compared to healthy ones [7], reflecting epithelial damage and remodeling. Our results indicate that CF-AOs treated with curcumin displayed a decrease in cell mortality, when assessed by PI staining (Fig. 7D-E). Furthermore, as shown in Fig. 7F-G, treatment reduces wall thickness in CF AOs, denoting an improvement of cell integrity.

Altogether, these data support the potential of curcumin as a therapeutic for inflammatory lung damage in CF.



(caption on next page)

Fig. 4. NRF2 activation by curcumin normalizes inflammation in *cfr*-depleted zebrafish. (A) Control MO and *cfr* MO were pre-treated with DMSO (as control) or curcumin before injury, then injured and immediately put back in treatments until analysis. (B) mRNA levels of *nrf2a* at 2 hpA (relative gene expression from at least 3 independent experiments performed in triplicates, Two-way ANOVA with Tukey's multiple comparisons test). (C) Neutrophil number at the wound at 2 hpA in control MO and *cfr* MO *TgBAC(mpx:EGFP)i114* (3 independent experiments, Two-way ANOVA with Tukey's multiple comparisons test). (D) Representative images of amputation-induced neutrophil mobilization in *cfr*-MO treated or not with curcumin (scale bars, 100 μ m). (E) Inhibition of *nrf2a* was carried out in CF animals by injecting the *nrf2a* morpholino. Neutrophil number at the wound at 2 hpA (3 independent experiments, Two-way ANOVA with Tukey's multiple comparisons test). (F) Schematic illustration of laser-mediated injury assay triggering ROS production by epithelial cells. (G-H) *cfr* MO are stained with CellROX®, treated, laser-injured, then ROS production was time-lapse imaged and quantified over 90 minutes by confocal microscopy. (G) ROS intensity at the wound site over the time course of inflammation. Line of best fit shown is calculated by linear regression. *P*-value shown is for the difference between the 2 slopes ($n = 12$, performed as 3 independent experiments). (H) Pseudocolored imaging of laser-injured caudal fin showing representative ROS production throughout inflammation. (I-M) mRNA levels of *duox*, *nqo1*, *hmxo1*, *cxcl8* and *il1 β* at 2 hpA (*duox*, *cxcl8* and *il1 β*) or 8 hpA (*nqo1* and *hmxo1*) determined by RT qPCR (relative gene expression from at least 3 independent experiments performed in triplicates, Two-way ANOVA with Tukey's multiple comparisons test). (N-O) *cfr* MO *Tg(il1b:eGFP-F)ump3* [19] were caudal fin amputated then the expression of *Il1 β* was observed and analyzed. Relative *Il1 β* intensity at 2hpA in *cfr* MO treated or not with curcumin ($n = 18$ from 3 independent experiments; Mann-Whitney *U* test) (N) and associated pseudocolored photomicrographs of injured tails (O) revealing *il1 β* expression at the wound-edge (scale bar, 100 μ m).

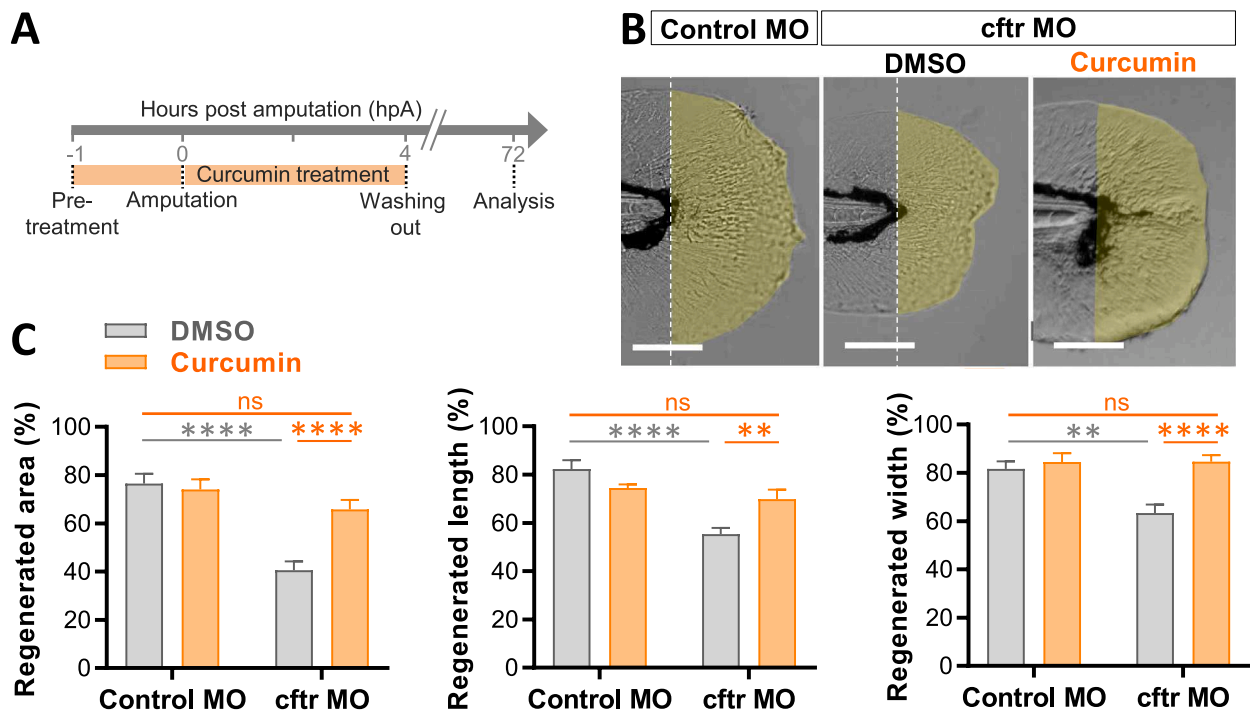


Fig. 5. Curcumin improves defective tissue repair capacity in *Cfr*-depleted animals. (A-C) Control MO and *cfr* MO were treated with DMSO or curcumin prior to caudal fin amputation procedure, then injured and immediately put back in treatments for 4 h. The potential of tissue repair was evaluated at 72 hpA. (B) Brightfield microscopy of injured caudal fin showing tissue regeneration in *cfr* MO treated with curcumin versus DMSO (scale bars, 100 μ m). (C) Measurement of regenerated caudal fin areas, lengths and widths following compounds exposure ($n = 20$, Two-way ANOVA, Tukey's multiple comparisons test).

4. Discussion

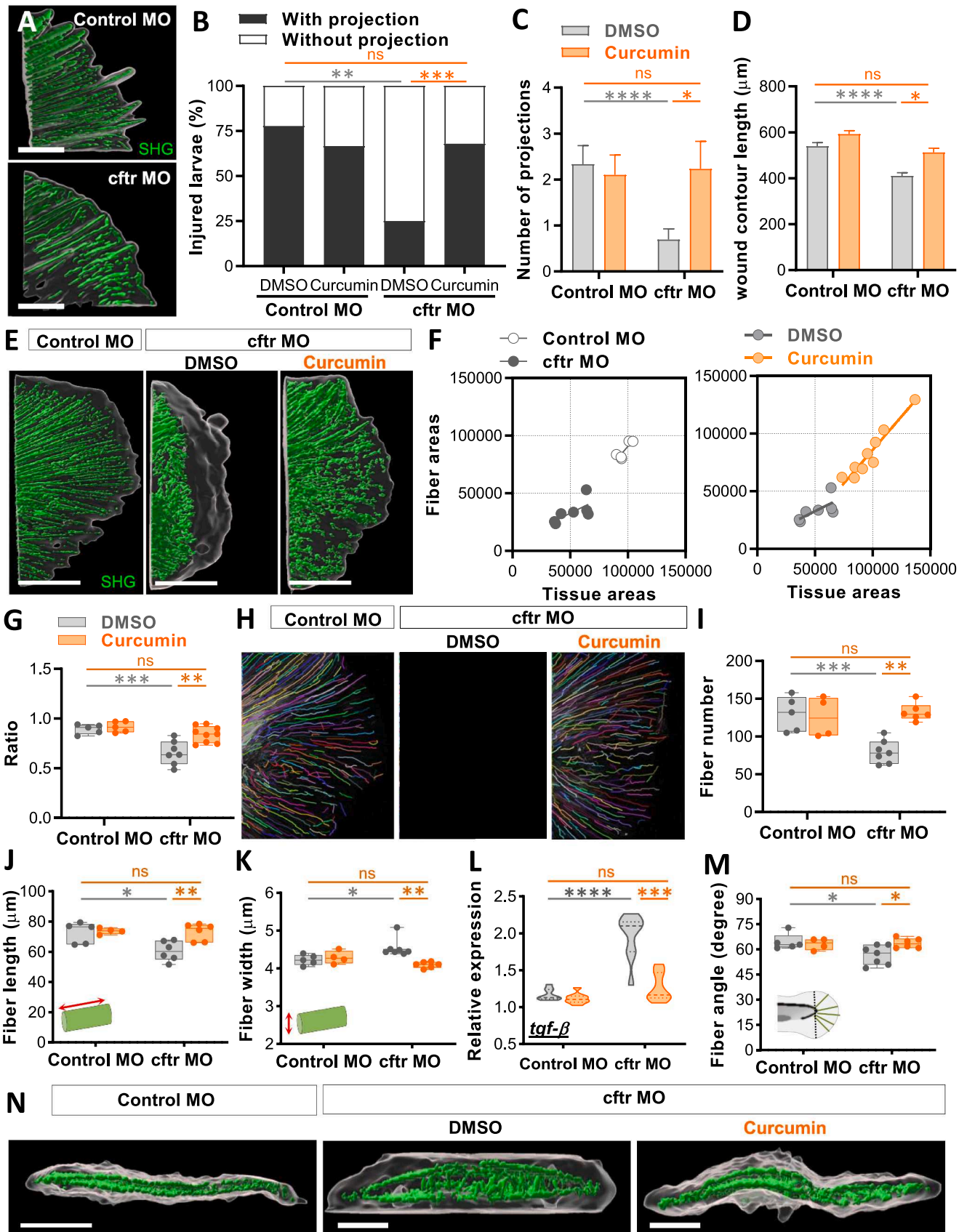
Over the last decade, research progresses have led to spectacular advances in the management of CF, in particular with CFTR correctors and potentiators correcting the basic defect of CFTR function [43]. However, excessive inflammation continues to be a major cause of lung injury and death in CF, indicating a continued need for novel strategies to prevent inflammation-related pulmonary decline.

Among the defective mechanisms specific to CF-related inflammatory pathogenesis, the NRF2 signaling pathway represent a promising target. Pharmacological activation of NRF2 in several models of CF results in decreased oxidative and pro-inflammatory responses [6–9], suggesting that restoring NRF2 activity might simultaneously prevent inflammation and tissue damage in CF individuals.

Here, using a combination of innovative animal and human models of CF, we sought to *i*) explore the role of NRF2 in CF-related inflammatory status and tissue damage and *ii*) determine the beneficial effect of curcumin on inflammation and tissue repair in the CF context. Our work identifies a role for NRF2 in neutrophilic inflammation (Fig. 2) and

tissue damage (Fig. 3) in CF. Importantly, we show that curcumin restores normal level of inflammation (Figs. 4 and 7) and tissue integrity (Figs. 5–7) in CF context, by rescuing NRF2 signaling.

Although evidence suggests that NRF2 defect in CF airways correlates with excessive generation of ROS and pro-inflammatory cytokines, the link between NRF2 dysfunction and CF-associated neutrophilic inflammation and tissue damage is not known. Our results reveal that loss of *Nrf2* signaling leads to an exuberant neutrophil response after injury in zebrafish (Fig. 2). It coincides with an excessive production of ROS and the pro-inflammatory cytokines IL8 and IL1 β , all well-known inducers of neutrophil mobilization. These data provide evidence that NRF2 pathway is instrumental to orchestrate neutrophil responses, likely by regulating oxidative and pro-inflammatory responses. Corroborating data from other CF models [6–9], *Cfr*-depleted zebrafish also exhibits impaired *Nrf2* signaling (Fig. 2). Our findings confirm that defective *Nrf2* contributes to the neutrophil-dominated inflammatory status in CF, since pharmacological NRF2 activation can block this effect in CF animals. The plausible explanation is that NRF2 dysfunction in CF leads to excessive production of ROS and pro-inflammatory cytokines by



(caption on next page)

Fig. 6. Curcumin reduces tissue damage by promoting remodeling of collagen fibers in CF zebrafish. Control MO and *cfr* MO were pre-treated with DMSO or curcumin prior to tail fin amputation procedure, then injured and immediately put back in treatments for 4 hrs. SHG microscopy of the regenerated tail fin was performed at 2 (A-D) or 3 dpA (E-K, M-N). (A) surface rendering of a 3D reconstruction showing tissue wound edge in the bright field and corresponding SHG imaging Z projections to reveal collagen projections in injured tails in control *versus* CF animals (scale bars, 25 μ m). (B-C) Proportion of larvae forming projections (B; n = 18–28 Fisher test) and the number of projections per larvae (C; n = 18–28, Two-way ANOVA, Tukey's multiple comparisons test), in fishes treated or not with curcumin. (D) Measurement of wound contour length in fishes treated or not with curcumin (n = 18–28 from 3 independent experiments, Two-way ANOVA with Tukey's multiple comparisons test). (E) 3D surface-rendered reconstruction of collagen fibers in regenerated tails to illustrate the spatial organization of fibers relative to regenerated tissue with tissue wound edge in the bright field and corresponding SHG imaging Z projections (scale bars, 100 μ m). (F) Areas of collagen fibers in Control MO *versus* *cfr* MO regenerated fin as a function of tissue areas (left), and areas of collagen fibers in the regenerated fin of CF fishes following DMSO or curcumin exposure as a function of tissue areas (right). (G) Graph showing the ratio of area devoid of SHG fibers (from fiber ends to wound edge) following fin amputation. Ratios were determined by measuring the areas devoid of SHG fibers normalize with total regenerated tissue from F. (H) CT-FIRE-generated projections of SHG imaging of collagen fibers in the tail fin showing changes in organization of collagen fibers during tissue repair process. (I-K) Graphs showing quantitation of fiber number (I), length (J), width (K) as determined using the CT-FIRE fiber analysis software (3 independent experiments, Two-way ANOVA with Tukey's multiple comparisons test). (L) mRNA levels of the pro-fibrotic cytokine *tgf- β* at 3dpA (RT qPCR relative gene expression from at least 3 independent experiments performed in triplicates, Two-way ANOVA with Tukey's multiple comparisons test). (M) Graphs showing quantitation of fiber angle determined with the CT-FIRE fiber analysis software (3 independent experiments, Two-way ANOVA with Tukey's multiple comparisons test). (N) 3D reconstruction from fin in cross section view revealing the spatial organization between tissue and the fibers (scale bars, 100 μ m), with abnormal fibbers extrusions found within the space between the 2 layers of collagen fibers.

epithelia in response to infections or injury (or inherent to CFTR mutations), which in turn, cause exuberant neutrophil influx in airways.

Consistent with previous studies suggesting a role for NRF2 in tissue repair [38], we show that zebrafish lacking *Nrf2* exhibit incomplete tail fin regrowth post-amputation, associated with disrupted collagen fiber formation and cell damage (Fig. 3). Ablation of neutrophil in *Nrf2a*-depleted animals partially rescues tissue repair, suggesting that neutrophilic inflammation is not the only cause of defective tissue repair in this context, and thus indicates that additional NRF2-mediated mechanisms are likely to participate in tissue repair processes. Similarly, we previously reported that *Cfr*-depleted zebrafish had abnormal tissue repair, partly due to neutrophilic inflammation [4]. This also appears to be NRF2 dependent, since activation of NRF2 signaling improves tissue repair in CF zebrafish (Figs. 5–7).

Overall, these findings demonstrate the role of deleterious changes in NRF2 activity in CF-related inflammation and tissue damage, and thus provide a rationale for targeting this pathway to prevent inflammatory damage in CF. Curcumin, primary constituent in turmeric derived from *Curcuma longa* rhizomes, is a potent activator of the NRF2 signaling pathway with anti-inflammatory, antioxidant and anti-infective therapeutic properties [44]. We confirm that NRF2 activity is restored by curcumin in both *Cfr*-depleted zebrafish and CF-AOs (Figs. 4 and 7). NRF2 is activated by stress [45]; KEAP1 allows NRF2 to escape degradation, accumulate within the cell, and translocate to the nucleus, where it can bind to AREs promoting antioxidant and anti-inflammatory transcription programs. Interestingly, despite the large amounts of ROS produced in CF airways, NRF2 signaling fails to be activated and translocated to the nucleus and is rapidly degraded in CF [6,8]. Notably, several mechanisms could be proposed to explain the stimulating action of curcumin on NRF2 in a context of CF [12,46]: by inhibiting KEAP1, by affecting the upstream mediators of NRF2 influencing the expression of *NRF2* and target genes, and/or by improving the nuclear translocation of NRF2.

Our findings indicate that curcumin can reduce CF inflammation *in vivo* and *ex vivo* by rebalancing excessive generation or inefficient detoxification of ROS, as well as elevated expression of *IL8* and *IL1 β* (Figs. 4 and 7). Consequently, curcumin alleviates CF-mediated neutrophilia. While curcumin has multiple effects and modes of action [44], we show that ablation of *Nrf2* signaling in CF zebrafish abolishes the protective effect of curcumin on inflammation. Although we cannot exclude the possibility that curcumin modulates additional mechanisms to reduce inflammation, our conclusions provide evidence that curcumin prevents CF-mediated inflammation *via* activating the NRF2 signaling pathway.

Since curcumin is well-tolerated [47], these findings could have significant therapeutic implications for targeting the pulmonary inflammation in CF, and thus may serve as supplements to current

therapeutic strategies or be an alternative to existing anti-inflammatory approaches. These data also suggest that curcumin may have beneficial effects on the extrapulmonary co-morbidities occurring in people with CF, such as digestive cancers [48], pancreatitis and diabetes [49]. While CF is principally characterized by pulmonary disease, CF-related diabetes resulting from pancreatic islets destruction involving inflammation is a common feature among the individuals with CF and is associated with accelerated lung decline and increased mortality [50, 51]. Importantly, an insufficient *Nrf2* activity is often associated with the etiology of diabetes and has been involved in the development of oxidative stress and inflammatory state in diabetic people [52]. Interestingly, NRF2 activation protects mouse model of diabetes from ROS-induced damage [53], suggesting that targeting NRF2-modulated ROS production might show promise in the treatment of pancreas destruction in a context of CF. Thus, having shown promising results in the treatment of diabetes [54], by reducing inflammation, curcumin might also prevent diabetes in CF individuals.

In CF, excessive inflammation disrupts airways integrity, leading to abnormal tissue remodeling and increased accumulation of ECM components which can give rise to fibrosis [55]. Our findings indicate that curcumin improves tissue repair in CF zebrafish, by reducing tissue damage and fibrotic phenotypes (Figs. 5–6). The amelioration of tissue integrity is also observed in CF-AOs, associated with reduction of cell mortality and aberrant tissue remodeling (Fig. 7), demonstrating that curcumin might prevent lung damage in people with CF. We have not yet identified the molecular events downstream of curcumin treatment in tissue repair and remodeling and how these might regulate collagen deposition. Modulation of macrophage [56] and fibroblast activities [57], two important cell populations in tissue repair processes, including collagen deposition, could be plausible cellular targets.

Increasing evidence, including our previous works, demonstrates that hyper-susceptibility to infections in CF would be in part linked to defective bactericidal activities in professional phagocytes, directly caused by CFTR dysfunction [15,58,59]. Interestingly, several studies indicate that NRF2 signaling pathway also plays a role in immune defense against pathogens [60]. A defect in NRF2 increases susceptibility to several CF-related bacteria, including *Pseudomonas aeruginosa* [60, 61], *Staphylococcus aureus* [62] and the mycobacterial species *Mycobacterium avium* [63] and *Mycobacterium abscessus* [64]), suggesting this could account for the infection phenotype in CF. Further investigations are needed to determine how CFTR/NRF2 interactions regulate antibacterial defenses and how this defective axis contributes to increased susceptibility to infections in CF.

Anti-inflammatory therapies must be carefully studied to minimize the risk of impeding host immune defenses and thus worsening infections, as we recently observed with roscovitine [21]. We showed that sulforaphane, another activator of NRF2, increases the killing

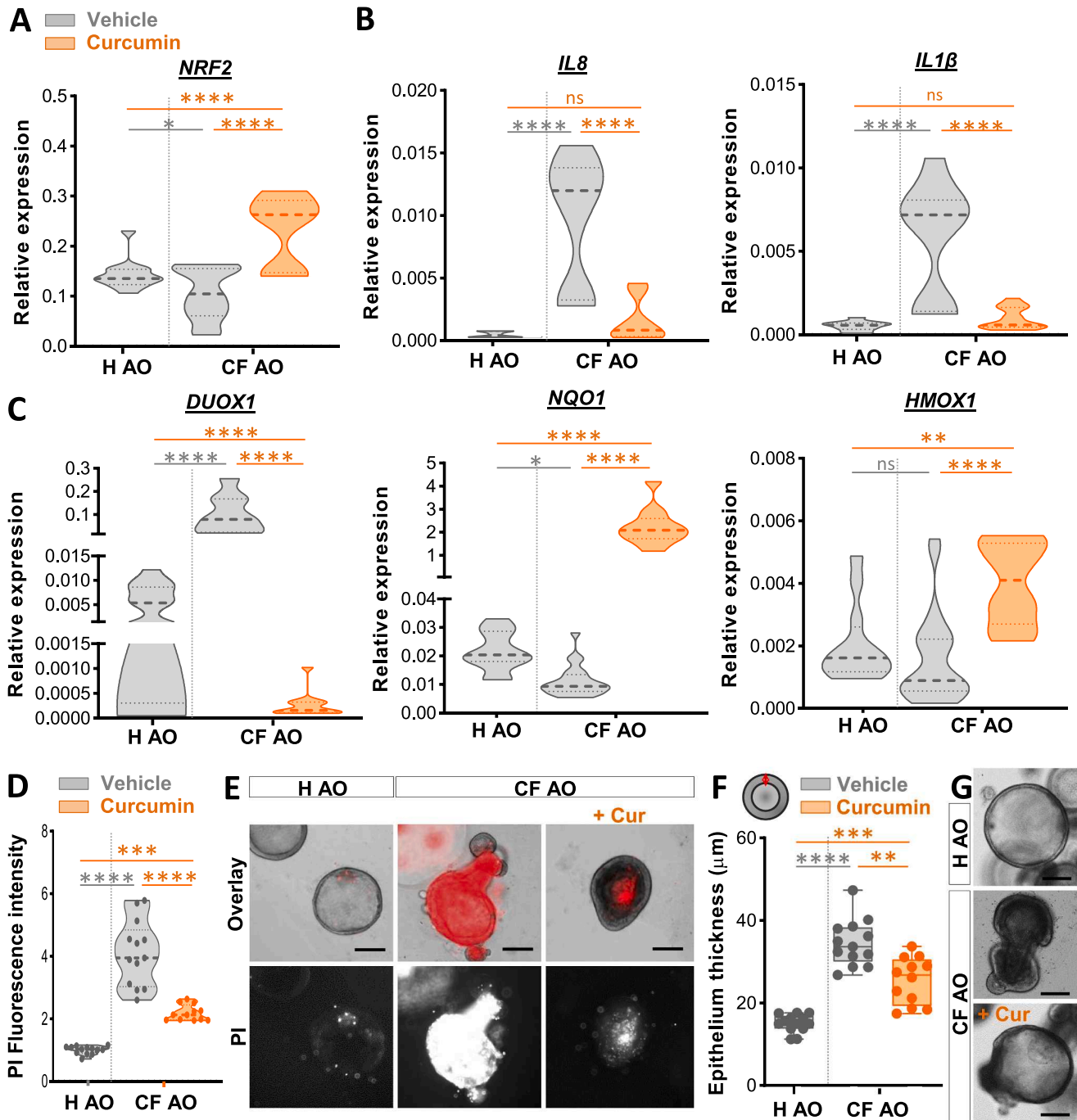


Fig. 7. Treatment with curcumin alleviates inflammatory state and tissue damage in human CF airway organoid. (A-C) Healthy or CF airway organoids (AOs) were incubated with vehicle (DMSO) control or 30 μM curcumin for 1 day. Gene expression levels of *NRF2* (A), the pro-inflammatory cytokines *IL8* and *IL1 β* (B), and the oxidative stress-related gene *DUOX1* and the *NRF2*-activated genes *NQO1* and *HMOX1* (D) were determined by RT qPCR (relative gene expression from at least 3 independent experiments performed in triplicates, ANOVA with Tukey's multiple comparisons test). (D-E) Cell death analysis in AOs treated with vehicle (DMSO) control or 30 μM curcumin for 4 days. Mean fluorescence intensity quantification of the propidium iodide (PI) incorporation (D) and representative images (scale bars, 300 μm) (E) in healthy and CF-AOs treated or not with curcumin ($n = 12-13$, from 3 independent experiments, Two-way ANOVA with Tukey's multiple comparisons test). (F-G) Quantification of the epithelial thickness ($n = 12-13$, from 3 independent experiments, ANOVA with Tukey's multiple comparisons test) (F) and representative images (scale bars, 300 μm) (G) in healthy and CF-AOs treated or not with 30 μM of curcumin for 4 days.

M. abscessus [7,65], suggesting that activation of *NRF2* might be an useful pharmacological approach for CF-associated defects in bacterial clearance. Hypothesizing that a decrease in *NRF2* signaling in people with CF hampers their ability to defend against pathogens, it could be interesting to test whether activation of *NRF2* by curcumin restores antimicrobial defense in CF. Moreover, while curcumin inhibits virulence factors in *P. aeruginosa*, such as the formation of biofilm or

pyocyanin biosynthesis, gene involved in quorum sensing [66], the antibiogenic synergic action of this compound also improves the activity of antibacterial agents against *S. aureus* [67], *M. abscessus* [68] and *P. aeruginosa* [69]. These results may have significant therapeutic implications for potentially targeting inflammation and improving host immunity to infections in CF.

Because the low bioavailability of curcumin, associated with its poor

solubility and absorption in free form in the gastrointestinal tract and its rapid biotransformation to inactive metabolites, there is a debate on its effectiveness and utility as a health-promoting compound [44]. However, this study was conducted with a free molecule, thus supporting its therapeutic and protective effects in the management of inflammation and tissue damage in CF. With the availability of highly bioavailable curcumin formulations [70], it should be now possible to exploit the full activities and benefits of curcumin in CF, and clinical trials will be necessary to confirm its effects in humans.

5. Conclusion

To conclude, our findings indicate that rescuing NRF2 using curcumin may be a targeted therapeutic strategy to both mitigate inflammation and restore tissue repair, and thus prevent inflammatory damage in individuals with CF.

Funding sources

This study was supported by the Horizon 2020 Research and Marie Skłodowska-Curie Innovation Framework Program (H2020-MSCA-IF-2016, CFZEBRA (751977); AB), the Fondation pour la Recherche Médicale (ARF201909009156; AB), the FC3R through the ZFishforCF-Care project (22FC3R-017; AB), the CF Trust (Workshop funding (160161); Strategic Research Centre SRC018; AB, RAF and SAR), the Vaincre La Mucoviscidose and Grégory Lemarchal Foundations (RF20240503516/1/1/101 for AB and RF20210502852/1/1/48 for CC and SAL-I). LY is supported by the Horizon 2020 Program Marie Skłodowska-Curie Innovative Training Network (H2020-MSCA-ITN-2020, INFLANET (955576)).

CRedit authorship contribution statement

Freteaud Maxence: Writing – review & editing, Visualization, Methodology, Investigation, Formal analysis. **Cornélie Sarahdja:** Writing – review & editing, Visualization, Investigation. **Floto Andres:** Writing – review & editing, Funding acquisition. **Herrmann Jean-Louis:** Writing – review & editing. **Bureau Charlotte:** Visualization, Formal analysis. **Yatime Laure:** Writing – review & editing, Visualization, Validation, Methodology, Investigation, Funding acquisition, Formal analysis. **Cougoule Céline:** Writing – review & editing, Visualization, Validation, Supervision, Methodology, Investigation, Funding acquisition, Formal analysis. **Bernut Audrey:** Writing – review & editing, Writing – original draft, Visualization, Validation, Supervision, Resources, Project administration, Methodology, Investigation, Funding acquisition, Formal analysis, Data curation, Conceptualization. **Renshaw Stephen:** Writing – review & editing, Funding acquisition. **Langevin Christelle:** Writing – review & editing, Visualization, Validation, Supervision, Methodology, Investigation, Formal analysis. **Leon-Icaza Stephen:** Writing – review & editing, Visualization, Methodology, Investigation, Formal analysis.

Author's Contributions

AB conceived the project, designed experiments, analyzed data and wrote the manuscript with input from SAL-I, MF, LY, RAF, SAR, J-LH, CL and CC. LY performed structural analyses. SAL-I and CC were responsible for the ex vivo testing in organoid models. MF and CL performed SHG imaging. SC, CB and AB performed zebrafish experiments. CL, CC and AB guided and supervised the work. All authors contributed to the article and approved the submitted version.

Declaration

Some of the results of this work have been reported in the form of a preprint (<https://doi.org/10.1101/2024.03.17.585384>).

Declaration of Competing Interest

The authors have no conflicts of interest to declare. All co-authors have seen and agree with the contents of the manuscript and there is no financial interest to report. We certify that the submission is original work and is not under review at any other publication.

Acknowledgments

We acknowledge the INRAE Infectiology of Fishes and Rodents Facility (IERP-UE907, Jouy-en-Josas Research Center, France doi.org/10.15454/1.5572427140471238E12) and the ZEFIX-Lphi (ZEBraFish and Xenopus platform, Lphi, University of Montpellier) fish facilities, and Dimitri Rigaudeau, Penelope Simon, Catherine Gonzalez and Victor Goulian for zebrafish maintenance and care, with a special thanks to Magalie Bouvet for technical assistance. IERP Facility belongs to the National Distributed Research Infrastructure for the Control of Animal and Zoonotic Emerging Infectious Diseases through In Vivo Investigation (EMERG'IN DOI: doi.org/10.15454/90CK-Y371). We thank the IERP for giving access to their injection platforms, the zebrafish phenotyping platform of IERP and imaging facility of MRI (Montpellier Ressources Imagerie), and Elodie Jublanc and Vicki Diakou for their assistance. We also thank Philippe Clair, the manager of the quantitative PCR facility of the University of Montpellier. Finally, we thank the University of Sheffield, the University of Versailles Saint-Quentin, the University of Montpellier, the animal health division of INRAE and the University of Toulouse for support.

Appendix A. Supporting information

Supplementary data associated with this article can be found in the online version at doi:10.1016/j.biopha.2025.117957.

References

- 1 J.S. Elborn, Cystic fibrosis, *Lancet (Lond., Engl.)* 388 (2016) 2519–2531.
- 2 C. McCarthy, Emmet O'Brien, M. Pohl, K. Reeves, E.P. McElvaney, NG. Airway inflammation in cystic fibrosis, *Eur. Respir. Monogr.* 64 (2014) 14–31.
- 3 D.P. Nichols, J.F. Chmiel, Inflammation and its genesis in cystic fibrosis, *Pedia Pulmonol.* (2015).
- 4 A. Bernut, C.A. Loynes, R.A. Floto, S.A. Renshaw, Deletion of cfr leads to an Excessive Neutrophilic Response and Defective Tissue Repair in a Zebrafish Model of Sterile Inflammation, *Front Immunol.* 11 (2020) 1733.
- 5 A.G. Ziady, J. Hansen, Redox balance in cystic fibrosis, *Int J. Biochem Cell Biol.* (2014).
- 6 J. Chen, M. Kinter, S. Shank, C. Cotton, T.J. Kelley, A.G. Ziady, Dysfunction of Nrf2 in CF epithelia leads to excess intracellular H₂O₂ and inflammatory cytokine production, *PLoS One* 3 (2008).
- 7 S.A. Leon-Icaza, S. Bagayoko, R. Vergé, N. Iakobachvili, C. Ferrand, T. Aydogan, et al., Druggable redox pathways against Mycobacterium abscessus in cystic fibrosis patient-derived airway organoids, in: H.I. Boshoff (Ed.), *PLOS Pathog.* 19, 2023 e1011559.
- 8 A.G. Ziady, A. Sokolow, S. Shank, D. Corey, R. Myers, S. Plafker, et al., Interaction with CREB binding protein modulates the activities of Nrf2 and NF-κB in cystic fibrosis airway epithelial cells, *Am. J. Physiol. - Lung Cell Mol. Physiol.* 302 (2012).
- 9 D.C. Borcherding, M.E. Siefert, S. Lin, J. Brewington, H. Sadek, J.P. Clancy, et al., Clinically approved CFTR modulators rescue Nrf2 dysfunction in cystic fibrosis airway epithelia, *J. Clin. Invest.* 129 (2019).
- 10 S.M.U. Ahmed, L. Luo, A. Namani, X.J. Wang, X. Tang, Nrf2 signaling pathway: Pivotal roles in inflammation, *Biochim Biophys. Acta - Mol. Basis Dis.* (2017).
- 11 A.M. Cantin, D. Hartl, M.W. Konstan, J.F. Chmiel, Inflammation in cystic fibrosis lung disease: Pathogenesis and therapy, *J. Cyst. Fibros.* (2015).
- 12 M. Ashrafizadeh, Z. Ahmadi, R. Mohammadinejad, T. Farkhondeh, S. Samarghandian, Curcumin Activates the Nrf2 Pathway and Induces Cellular Protection Against Oxidative Injury, *Curr. Mol. Med.* 20 (2019).
- 13 M.E. Egan, M. Pearson, S.A. Weiner, V. Rajendran, D. Rubin, J. Glöckner-Pagel, et al., Curcumin, a Major Constituent of Turmeric, Corrects Cystic Fibrosis Defects, *Science* 304 (2004) 80.
- 14 A.L. Berger, C.O. Randak, L.S. Ostedgaard, P.H. Karp, D.W. Vermeer, M.J. Welsh, Curcumin stimulates cystic fibrosis transmembrane conductance regulator Cl⁻ channel activity, *J. Biol. Chem.* 280 (2005).
- 15 A. Bernut, C. Dupont, N.V. Ogryzko, A. Neyret, J.L. Herrmann, R.A. Floto, et al., CFTR Protects against Mycobacterium abscessus Infection by Fine-Tuning Host Oxidative Defenses, *Cell Rep.* 26 (2019) 1828–1840.e4.

- 16 J.A. Lister, C.P. Robertson, T. Lepage, S.L. Johnson, D.W. Raible, Nacre Encodes a Zebrafish Microphthalmia-Related Protein That Regulates Neural-Crest-Derived Pigment Cell Fate, *Development* 126 (1999) 3757–3767.
- 17 R.L. Lamason, M.A.P.K. Mohideen, J.R. Mest, A.C. Wong, H.L. Norton, M.C. Aros, et al., Genetics: SLC24A5, a putative cation exchanger, affects pigmentation in zebrafish and humans, *Science* (80-) 310 (2005) 1782–1786.
- 18 S.A. Renshaw, C.A. Loynes, D.M.I. Trushell, S. Elworthy, P.W. Ingham, M.K. B. Whyte, Atransgenic zebrafish model of neutrophilic inflammation, *Blood* 108 (2006) 3976–3978.
- 19 M. Nguyen-Chi, Q.T. Phan, C. Gonzalez, J.F. Dubremetz, J.P. Levrard, G. Lutfalla, Transient infection of the zebrafish notochord with *E. coli* induces chronic inflammation, *DMM Dis. Model Mech.* 7 (2014) 871–882.
- 20 K. Ellis, J. Bagwell, M. Bagnat, Notochord vacuoles are lysosome-related organelles that function in axis and spine morphogenesis, *J. Cell Biol.* 200 (2013).
- 21 V. Le Moigne, D. Rodriguez Rincon, S. Glatigny, C.M. Dupont, C. Langevin, A. Ait Ali Said, et al., Roscovitine Worsens Mycobacterium abscessus Infection by Reducing DUOX2-mediated Neutrophil Response, *Am. J. Respir. Cell Mol. Biol.* 66 (2022) 439–451.
- 22 Westerfield M. *The Zebrafish Book. A Guide for the Laboratory Use of Zebrafish (Danio rerio)*, 5th Edition. Univ Oregon Press Eugene 2007;
- 23 A.R. Timme-Laragy, S.I. Karchner, D.G. Franks, M.J. Jenny, R.C. Harbeitner, J. V. Goldstone, et al., Nrf2b, novel zebrafish paralog of oxidant-responsive transcription factor NF-E2-related factor 2 (NRF2), *J. Biol. Chem.* 287 (2012) 4609–4627.
- 24 N. Palha, F. Guivel-Benhassine, V. Briolat, G. Lutfalla, M. Sourisseau, F. Ellett, et al., Real-Time Whole-Body Visualization of Chikungunya Virus Infection and Host Interferon Response in Zebrafish, *PLoS Pathog.* 9 (2013).
- 25 P. Niethammer, C. Grabher, A.T. Look, T.J. Mitchison, A tissue-scale gradient of hydrogen peroxide mediates rapid wound detection in zebrafish, *Nature* 459 (2009) 996–999.
- 26 G. Lutfalla, G. Uze, [19] Performing Quantitative Reverse-Transcribed Polymerase Chain Reaction Experiments, *Methods Enzym.* (2006).
- 27 D. LeBer, J.M. Squirrel, C. Freisinger, J. Rindy, N. Golenberg, G. Frecentese, et al., Damage-induced reactive oxygen species regulate vimentin and dynamic collagen-based projections to mediate wound repair, *Elife* 7 (2018).
- 28 Y. Liu, A. Keikhosravi, G.S. Mehta, C.R. Drifka, K.W. Eliceiri, Methods for quantifying fibrillar collagen alignment, *Methods Mol. Biol.* (2017).
- 29 N. Sachs, A. Papaspypopoulos, D.D. Zomer-van Ommen, I. Heo, L. Böttinger, D. Klay, et al., Long-term expanding human airway organoids for disease modeling, *EMBO J.* 38 (2019).
- 30 N. Iakobachvili, S.A. Leon-Icaza, K. Knoop, N. Sachs, S. Mazères, R. Simeone, et al., Mycobacteria–host interactions in human bronchiolar airway organoids, *Mol. Microbiol* 117 (2022) 682–692.
- 31 J. Jumper, R. Evans, A. Pritzel, T. Green, M. Figurnov, O. Ronneberger, et al., Highly accurate protein structure prediction with AlphaFold, *Nature* 596 (2021).
- 32 P. Emsley, K. Cowtan, Coot: Model-building tools for molecular graphics, *Acta Crystallogr Sect. D. Biol. Crystallogr* 60 (2004).
- 33 F. Madeira, M. Pearce, A.R.N. Tivey, P. Basutkar, J. Lee, O. Edbali, et al., Search and sequence analysis tools services from EMBL-EBI in 2022, *Nucleic Acids Res* 50 (2022).
- 34 C.S. Bond, A.W. Schüttelkopf, ALINE: A WYSIWYG protein-sequence alignment editor for publication-quality alignments, *Acta Crystallogr Sect. D. Biol. Crystallogr* 65 (2009).
- 35 M. Kobayashi, K. Itoh, T. Suzuki, H. Osanai, K. Nishikawa, Y. Katoh, et al., Identification of the interactive interface and phylogenetic conservation of the Nrf2-Keap1 system, *Genes Cells* 7 (2002).
- 36 P. Niethammer, C. Grabher, A.T. Look, T.J. Mitchison, A tissue-scale gradient of hydrogen peroxide mediates rapid wound detection in zebrafish, *Nature* 459 (2009) 996–999.
- 37 E.H. Kobayashi, T. Suzuki, R. Funayama, T. Nagashima, M. Hayashi, H. Sekine, et al., Nrf2 suppresses macrophage inflammatory response by blocking proinflammatory cytokine transcription, *Nat. Commun.* 7 (2016).
- 38 P. Hiebert, S. Werner, Targeting NRF2 to promote epithelial repair, *Biochem Soc. Trans.* (2023).
- 39 P. Hiebert, The Nrf2 transcription factor: A multifaceted regulator of the extracellular matrix, *Matrix Biol.* (2021).
- 40 K.R. Schiller, P.J. Maniak, O'Grady SM. Cystic fibrosis transmembrane conductance regulator is involved in airway epithelial wound repair, *Am. J. Physiol. - Cell Physiol.* 299 (2010).
- 41 W.T. Harris, D.R. Kelly, Y. Zhou, D. Wang, M. Macewen, J.S. Hagood, et al., Myofibroblast Differentiation and Enhanced Tgf- β Signaling in Cystic Fibrosis Lung Disease, *PLoS One* 8 (2013).
- 42 J. Kuroda, T. Itabashi, A.H. Iwane, T. Aramaki, S. Kondo, The Physical Role of Mesenchymal Cells Driven by the Actin Cytoskeleton Is Essential for the Orientation of Collagen Fibrils in Zebrafish Fins, *Front Cell Dev. Biol.* 8 (2020).
- 43 E. Bardin, A. Pastor, M. Semeraro, A. Golec, K. Hayes, B. Chevalier, et al., Modulators of CFTR. Updates on clinical development and future directions, *Eur. J. Med Chem.* 213 (2021).
- 44 X.Y. Xu, X. Meng, S. Li, R.Y. Gan, Y. Li, H. Bin Li, Bioactivity, health benefits, and related molecular mechanisms of curcumin: Current progress, challenges, and perspectives, *Nutrients* (2018).
- 45 L. Baird, M. Yamamoto, The Molecular Mechanisms Regulating the KEAP1-NRF2 Pathway, *Mol. Cell Biol.* 40 (2020).
- 46 N. Robledinos-Antón, R. Fernández-Ginés, G. Manda, A. Cuadrado, Activators and Inhibitors of NRF2: A Review of Their Potential for Clinical Development, *Oxid. Med Cell Longev.* (2019).
- 47 S.J. Hewlings, D.S. Kalman, Curcumin: A review of its effects on human health, *Foods* (2017).
- 48 A. Yamada, Y. Komaki, F. Komaki, D. Micic, S. Zullo, A. Sakuraba, Risk of gastrointestinal cancers in patients with cystic fibrosis: a systematic review and meta-analysis, *Lancet Oncol.* 19 (2018).
- 49 A. Granados, C.L. Chan, K.L. Ode, A. Moheet, A. Moran, R. Holl, Cystic fibrosis related diabetes: Pathophysiology, screening and diagnosis, *J. Cyst. Fibros.* 18 (2019) S3–S9.
- 50 R.L. Hull, R.L. Gibson, S. McNamara, G.H. Deutsch, C.L. Fligner, C.W. Frevert, et al., Islet interleukin-1 β immunoreactivity is an early feature of cystic fibrosis that may contribute to β -cell failure, *Diabetes Care* 41 (2018).
- 51 B.J. Prentice, A. Jaffe, S. Hameed, C.F. Verge, S. Waters, J. Widger, Cystic fibrosis-related diabetes and lung disease: An update, *Eur. Respir. Rev.* (2021).
- 52 M. Dodson, A. Shakya, A. Anandhan, J. Chen, J.G.N. Garcia, D.D. Zhang, NRF2 and Diabetes: The Good, the Bad, and the Complex, *Diabetes* 71 (2022).
- 53 R. Rajappa, D. Sireesh, M.B. Salai, K.M. Ramkumar, S. Sarvajayakesavulu, S.R. V. Madhupantula, Treatment with naringenin elevates the activity of transcription factor Nrf2 to protect pancreatic β -cells from streptozotocin-induced diabetes in vitro and in vivo, *Front Pharm.* 9 (2019).
- 54 C. Quispe, J. Herrera-Bravo, Z. Javed, K. Khan, S. Raza, Z. Gulsunoglu-Konuskan, et al., Therapeutic Applications of Curcumin in Diabetes: A Review and Perspective, *Biomed. Res Int* (2022).
- 55 N. Regamey, P.K. Jeffery, E.W.F.W. Alton, A. Bush, J.C. Davies, Airway remodelling and its relationship to inflammation in cystic fibrosis, *Thorax* (2011).
- 56 L. Wang, C. He, Nrf2-mediated anti-inflammatory polarization of macrophages as therapeutic targets for osteoarthritis, *Front Immunol.* (2022).
- 57 P. Hiebert, A. Martyts, J. Schwestermann, K. Janke, J. Hafner, P. Boukamp, et al., Activation of Nrf2 in fibroblasts promotes a skin aging phenotype via an Nrf2-miRNA-collagen axis, *Matrix Biol.* 113 (2022).
- 58 D. Hartl, A. Gaggari, E. Bruscia, A. Hector, V. Marcos, A. Jung, et al., Innate immunity in cystic fibrosis lung disease, *J. Cyst. Fibros.* 11 (2012) 363–382.
- 59 A. Weimann, A. Dinan, C. Ruis, A. Bernut, S. Pont, K. Brown, J. Ryan, L. Santos, L. Ellison, E. Ukor, A. Pandurangan, S. Krokowski, T. Blundell, P. Harrison, S. T. Peacock, J.F.A. Parkhill, Evolution and host-specific adaptation of *Pseudomonas aeruginosa*, *Science* 80 (2024).
- 60 C.J. Harvey, R.K. Thimmulappa, S. Sethi, X. Kong, L. Yarmus, R.H. Brown, et al., Targeting Nrf2 signaling improves bacterial clearance by alveolar macrophages in patients with COPD and in a mouse model, *Sci. Transl. Med* 3 (2011).
- 61 R. Thimmulappa, T. Sussan, S. Biswal, Deficiency of NRF2 predisposes mice to *Pseudomonas aeruginosa* induced pneumonia, *FASEB J.* 22 (2008).
- 62 J. Athale, A. Ulrich, N. Chou MacGarvey, R.R. Bartz, K.E. Welty-Wolf, H.B. Suliman, et al., Nrf2 promotes alveolar mitochondrial biogenesis and resolution of lung injury in *Staphylococcus aureus* pneumonia in mice, *Free Radic. Biol. Med* 53 (2012) 1584–1594.
- 63 M. Nakajima, M. Matsuyama, M. Kawaguchi, T. Kiwamoto, Y. Matsuno, Y. Morishima, et al., Nrf2 regulates granuloma formation and macrophage activation during *Mycobacterium avium* infection via mediating nramp1 and ho-1 expressions, *MBio* 12 (2021).
- 64 A. Fortuin, M. Frétau, M. Lagune, L. Yatime, S. Renshaw, A. Floto, et al., P235 Pharmacological activation of NRF2 has protective effects during *Mycobacterium abscessus* infection by promoting host defences and reducing inflammatory damage in the context of cystic fibrosis, *J. Cyst. Fibros.* 22 (2023) S137.
- 65 M. Bonay, A.-L. Roux, J. Floquet, Y. Retory, J.-L. Herrmann, F. Lofaso, et al., Caspase-independent apoptosis in infected macrophages triggered by sulfuraphane via Nrf2/p38 signaling pathways, *Cell Death Discov.* 1 (2015) 15022.
- 66 T. Rudrappa, H.P. Bais, Curcumin, a known phenolic from *Curcuma longa*, attenuates the virulence of *Pseudomonas aeruginosa* PAO1 in whole plant and animal pathogenicity models, *J. Agric. Food Chem.* 56 (2008).
- 67 S.Y. Teow, K. Liew, S.A. Ali, A.S.B. Khoo, S.C. Peh, Antibacterial Action of Curcumin against *Staphylococcus aureus*: A Brief Review, *J. Trop. Med* (2016).
- 68 E. Marini, M. Di Giulio, G. Magi, S. Di Lodovico, M.E. Cimarelli, A. Brenciani, et al., Curcumin, an antibiotic resistance breaker against a multiresistant clinical isolate of *Mycobacterium abscessus*, *Phyther Res* 32 (2018).
- 69 S. Bahari, H. Zeighami, H. Mirshahabi, S. Roudashti, F. Haghi, Inhibition of *Pseudomonas aeruginosa* quorum sensing by subinhibitory concentrations of curcumin with gentamicin and azithromycin, *J. Glob. Antimicrob. Resist* 10 (2017).
- 70 S.J. Stohs, O. Chen, S.D. Ray, J. Ji, L.R. Bucci, H.G. Preuss, Highly bioavailable forms of curcumin and promising avenues for curcumin-based research and application: A review, *Molecules* (2020).